

## Article

# Experimental Investigation of the Porous Free Zone of Silicon Cemented Layer Obtained through Pack Cementation

Mihai Ovidiu Cojocaru<sup>1,2</sup>, Mihai Branzei<sup>1,\*</sup> , Mircea Dan Morariu<sup>1</sup>, Cosmin Mihai Cotrut<sup>1</sup>   
and Daniela Dragomir<sup>3</sup>

<sup>1</sup> Department of Metallic Materials Science, Physical Metallurgy, Faculty of Materials Science and Engineering, University Politehnica of Bucharest, 060042 Bucharest, Romania

<sup>2</sup> Section IX-Materials Science and Engineering, Technical Sciences Academy of Romania, 030167 Bucharest, Romania

<sup>3</sup> Executive Unit for Financing Higher Education, Research, Development, and Innovation, 010987 Bucharest, Romania

\* Correspondence: mihai.branzei@upb.ro

**Abstract:** The development of a porous free zone of the silicon cemented layer represents a scientific and technical challenge. The limitation of the effects of the Kirkendall–Frenkel phenomena requires the right control of the thermochemical processing parameters (temperature, time, and chemical) and thorough knowledge of the related interaction with the specific elements of the metallic matrix of the thermochemically processed product. Through the experimental programming method, the individual and cumulated effects of the thermochemical processing parameters on (Fe–Armco) high-purity iron cemented by silicon in ferrosilicon (FeSi75C) powdered solid media have been quantified. It was concluded that ferrosilicon with silicon concentrations higher than 60% (FeSi75C) represents a redoubtable active component, especially in a temperature range higher than 1100 °C. In the layer cemented with silicon, the presence of nitrogen was also observed, as a direct consequence of the composition of the medium used for cementation. The presence of this element is the predominant result of the manifestation of the ionic phenomenon of adsorption. The correlations between these parameters and the dimension of the porous free zone of the silicon cemented layer in the vicinity of the thermochemically processed surface have been determined.

**Keywords:** silicon cementation in powdered solid media; diffusion porosity; Kirkendall–Frenkel effect; experimental programming; porous free zone; ionic mechanism of adsorption



**Citation:** Cojocaru, M.O.; Branzei, M.; Morariu, M.D.; Cotrut, C.M.; Dragomir, D. Experimental Investigation of the Porous Free Zone of Silicon Cemented Layer Obtained through Pack Cementation. *Metals* **2023**, *13*, 162. <https://doi.org/10.3390/met13010162>

Academic Editor: Hui Wang

Received: 20 October 2022

Revised: 8 December 2022

Accepted: 2 January 2023

Published: 12 January 2023



**Copyright:** © 2023 by the authors. Licensee MDPI, Basel, Switzerland. This article is an open access article distributed under the terms and conditions of the Creative Commons Attribution (CC BY) license (<https://creativecommons.org/licenses/by/4.0/>).

## 1. Introduction

Silicon pack cementation of parts ensures a significant increase in the corrosion resistance, refractivity, hardness, and wear resistance, or a sum of these properties, needed in exploitation for various component categories [1–3]. Silicon cementation of high-purity iron results in the formation of a solid solution of silicon in  $\alpha$ -Fe near the surface of the metal product being processed [4].

According to the Fe–Si phase equilibrium diagram, the diffusion layer often consists of the  $\alpha_1$  phase (solid solution based on a Fe<sub>3</sub>Si type compound) in the vicinity of the surface and the  $\alpha$  solid solution in depth, near the substrate. Consequently, the  $\alpha_1$  phase is the source of silicon, which ensures the saturation of the  $\alpha$  solid solution. The presence of alloying elements and carbon can influence both the growth kinetics of the silicon cemented layer and the porosity level.

The differences between the values of the diffusion coefficients of the various elements (for example, Fe and Si, respectively) between the movement rates of the flows of various species of atoms during the formation of the silicon cemented layer generate the initiation of the Kirkendall–Frenkel phenomena, with immediate consequences on diffusion porosity (the pores are based on diffusion phenomena and occur through vacancies).

Samsonov and Epik [5] characterize the siliconized layers obtained by cementation in solid, gaseous, and liquid media, respectively, starting from the first Russian author Dueva [6], showing that a layer with a thickness of 300–900 microns can be obtained, but at holding times of at least 10 h at 1100–1200 °C. Haslam and Carlsmith [7] mentioned in their paper that no evidence of cementation was observed under 1100 °C and above 1350 °C fusion occurred. Balandin and Kolpakov [8] showed in their paper that the use of a fluidized bed makes it possible to intensify considerably the processes of siliconizing. So, siliconizing in a fluidized bed is a promising process of thermochemical treatment for steels operating under conditions of corrosion, high temperatures, and wear resistance.

The siliconizing mechanism was investigated in 1954 by Fitzer [9]. At that time, ferrosilicon with up to 20% Si was used, with a thermochemical treatment temperature of 1500 °C and a holding time of 5 to 30 h. Thus, in addition to the expected effects, there were also unwanted effects, such as the increase and non-uniformity of the grain size, both in the siliconized layer and in the core of the part.

Representative in this regard is the cementation of high-purity iron by silicon, where the silicon diffusion in depth in the direction of  $\alpha_1 \rightarrow \alpha$  exceeds the iron diffusion rate in the opposite direction. Usually, the diffusion porosity appears locally in the  $\alpha_1$  phase wherein the unit of time and unit of volume enter a smaller number of iron atoms compared to the number of silicon atoms entered in the  $\alpha$  phase. In line with the experimental results obtained by several authors, among which is Lakhtin [1], when solid powdered mixtures are utilized for silicon cementation, in the absence of components with the role of dissipation and reduction of the tendency of sintering the active components  $\text{Al}_2\text{O}_3$ , the powder mixture becomes very active. In this regard, the probability of the formation of fragile and porous  $\alpha_1\text{-Fe}_3\text{Si}$  phase increases considerably. On the other hand, the introduction of the activator (halide) increases the probability of the appearance of fragile and porous zones of the  $\alpha_1$  phase. The decrease in the activity of the silicon cementation media by diminishing the proportion of the active part and the proportion of the activator (i.e.,  $\text{NH}_4\text{Cl}$ ) results in the equalization of the mutual diffusion coefficients and, implicitly, the decrease in the porosity. Seemingly contradictorily, the effects of the presence or absence of the different components of the media utilized for silicon cementation must be quantified; it is also important to determine the cumulated action of the effects of the groups of parameters—active component–activator, active component–temperature, active component–activator, component with the role of dispersion/ballast, etc. This objective can be achieved through experimental programming and subsequent statistical processing of the experimental data thus obtained.

Lakhtin et al. [1] recommended several measures to prevent the occurrence of diffusion porosity of the silicon cemented layer, as follows:

- Alloying of the metallic matrix (which is to be silicon cemented) with elements having lower melting temperatures and characterized by the high mobility of atoms.
- Simultaneous saturation of the surface with silicon and other elements with low diffusion mobility, e.g., chromium.
- The generation of pressure that is uniformly distributed on the surface of the thermochemically processed product, leading to significant diffusion of vacancies and pores to the surface of the product.

Currently, the only guarantee of ensuring a silicon cemented layer without porosity is given by the absence of the  $\alpha_1$  phase [1].

Based on these findings and considering that silicon cementation is applied to ensure high corrosion resistance, it becomes imperative to achieve a non-porous silicon cemented layer. This aim can be reached by silicon cementation of high-carbon steels, or for the case of low-carbon steels, which must maintain low carbon in the core, it is recommended to apply carbon cementation previously.

The purpose of the experimental research was to quantify the effects of the change in individual/combined technological parameters of the silicon cementation process on the growth kinetics of the porous-free zone (of the silicon cemented layer) adherent to the

thermochemically processed surface. The active part of the medium was FeSi powder, with a high silicon content (approximately 75%). The metallic matrix used for experiments was a high-purity iron matrix (Fe-ARMCO).

This allows us to clearly emphasize the changes in the phase composition and their morphological particularities generated strictly by the variation of the parameters with notable influence on the kinetics and phase composition. The porous-free zone of the silicon cemented layer was defined as being the distance between the metallic matrix-layer interface, which is noticeable metallographic, and the zone of the layer where the diffusion porosity occurs; its size has been adopted as the arithmetic means of 4-5 measurements.

The experimental research aimed at determining and quantifying the effects of the variation of thermal, temporal, and chemical parameters of the silicon cementation process in powdery solid media applied to high-purity iron on the growth kinetics of the silicon cemented layer, targeting the zone of the layer in contact with the metal matrix of which the dimension extends to the zone where the porosity occurs.

## 2. Materials and Methods

The multitude of factors that contribute to the formation of a dense silicon cemented layer adhering to the metallic matrix justified the decision to use the experimental programming method to quantify their individual and cumulated effects on the growth kinetics of the layer. The complete factorial programming method was initially adopted, after which we chose another type of programming in case the statistical verifications could not confirm the correctness of the selection of it. Silicon cementations were performed in powdered solid media with active components of ferrosilicon with 75% Si (FeSi75C). Alumina, the dissipation part, has played a key role in the avoidance of mutual sintering of the components of the powdery solid medium.  $\text{NH}_4\text{Cl}$  was the activator of the metal surface subjected to thermochemical processing. Furthermore, it was the supplier of components able to react with silicon in the medium (from FeSi), thus ensuring the surface's saturation with this element.

Chamber furnaces with automatic temperature regulation and control were used. The samples were packed in solid powder mixtures and positioned in refractory steel containers; the containers were sealed with clay, placed in the furnace at 200 °C, and heated with the furnace up to the holding temperature. After reaching the holding temperature, the containers were taken out and cooled freely in the air; the extraction of samples was realized for a temperature of the containers below 300 °C.

The characteristics of the components of powdered solid mixtures were as follows:

- Ferrosilicon (FeSi75C with 72–75% Si and below 0.1% C, with approximately 2% Al) produced by the Norwegian company FINNFJORD; particles with an average equivalent diameter of 40–50  $\mu\text{m}$ , subsequently grounded into ball mills to an average equivalent diameter of 3–4  $\mu\text{m}$ .
- Alumina powders ( $\text{Al}_2\text{O}_3 > 98.5\%$ ) are produced at Alum. S.A. Romania, fraction  $> 150 \mu\text{m}$  max. 10%; fraction  $< 45 \mu\text{m}$  max. 12%.
- Ammonium chloride ( $\text{NH}_4\text{Cl}$ ) of analytical purity, produced by SilverChemicals Romania.

The metallic materials used in the experimental research to highlight the studied aspects were high-purity iron (Fe-ARMCO), with the chemical composition as presented in Table 1 (determination made with a SPECTROLAB M10/76004135 spectrometer).

**Table 1.** The chemical composition of the high-purity iron (Fe-ARMCO).

| El.<br>% | C    | Si   | Mn   | P     | S     | Cu   | Ni   | Cr    | Mo    | V      | Al    | N     | Fe    |
|----------|------|------|------|-------|-------|------|------|-------|-------|--------|-------|-------|-------|
|          | 0.02 | 0.07 | 0.12 | 0.017 | 0.011 | 0.01 | 0.01 | 0.003 | 0.004 | 0.0005 | 0.006 | 0.008 | 99.70 |

The chemical composition of the metallic materials used in the research is presented in Table 1.

The investigation of the obtained results was realized by the use of:

- Vickers HV0.05 (50gf) hardness tests were performed on the NEOPHOT 21 microscope N1096 series.
- Optical Microscopy (OM) using a Zeiss Z1m Observer microscope-Axio Vision 4.8/038-12837.
- Scanning Electron Microscopy (SEM) using a TESCAN VEGA XMU 8 microscope and Philips XL30 ESEM TMP microscope.
- EDAX spectrometry (EDAX Sapphire type dispersive energy spectrometer with a resolution of 128 kV).
- XRF analyses performed on the SPECTRO xSORT device no. 143714 used for the additional verification of silicon concentration in the superficial layers of the silicon cemented Fe-ARMCO.

### 3. Results

A high corrosion-resistance level required for the parts utilized in the chemical and petrochemical industry can be ensured using silicon cementation and the development of a free porous zone of a silicon cemented layer tightly adhered to the substrate [10].

To highlight the individual and cumulative influence of the variation of the processing parameters, experimental programming was applied, considering the first-order programming-complete factorial experiment [11–15]. The reason for adopting the first-order programming is related to previous authors [10] arguing the limiting role of the penetration of the silicon atoms flux from outside to the inside of the diffusion zone and to the similarity between the dependencies: Layer growth kinetics–temperature and silicon diffusion coefficient–temperature. The aim was to clarify correlation regression equations, such as:

$$Y = \delta(\mu m) = b_0 + \sum_{\substack{i=1 \\ j=1 \\ k=1 \\ l=1}}^m b_{i,j,\dots} x_i, j,\dots + \sum_{\substack{i=1 \\ j=1 \\ k=1 \\ l=1}}^m b_{ij,ik;il,\dots} x_i x_j \dots x_i x_k \dots + \sum_{\substack{i=1 \\ j=1 \\ k=1 \\ l=1}}^m b_{ijk;ijl,\dots} x_i x_j x_k \dots \quad (1)$$

where:

$b_i; b_{ij}$ —the real coefficients of Equation (1).

$x_i; x_j$ —the coded values of the factors (independent parameters taken into analysis).

$Y$ —the real value of the dependent parameters (in the current situation,  $Y$  represents the dimension of the silicon cemented layer's dense, porous free, and adherent zone, in direct contact with the surface of the thermochemically processed product)—see example in Figure 1.

Metallographically, it is also confirmed that the associated effect of the variation of the proportion of the active component and the holding time at the thermochemical processing temperature, i.e., at high concentrations of the halides in the powdered solid media, on the growth kinetics of the free porous zone of the layer is significant. Thus, a decrease in the proportion of the active component by approximately 20% and an increase in the holding time at a certain temperature (1150 °C, in this case) by 400% (cond. exp. 4→cond. exp. 7) ensures an increase in the dimensions of the zone of interest of the silicon cemented with an average value of 52%, as it is shown in Figure 1.

To better understand how the independent parameters in the analysis (the processing temperature, holding time on temperature, the proportion of the active component—ferrosilicon, and the proportion of  $\text{NH}_4\text{Cl}$ ) influence the growth kinetics of the related zone of the silicon cemented layer, both the individual effects of the variation of these parameters ( $b_i x_i; b_j x_j \dots$ ) and the cumulated effects of these ( $b_{ij} x_i x_j; \dots b_{ijk} x_i x_j x_k \dots$ ) were calculated.

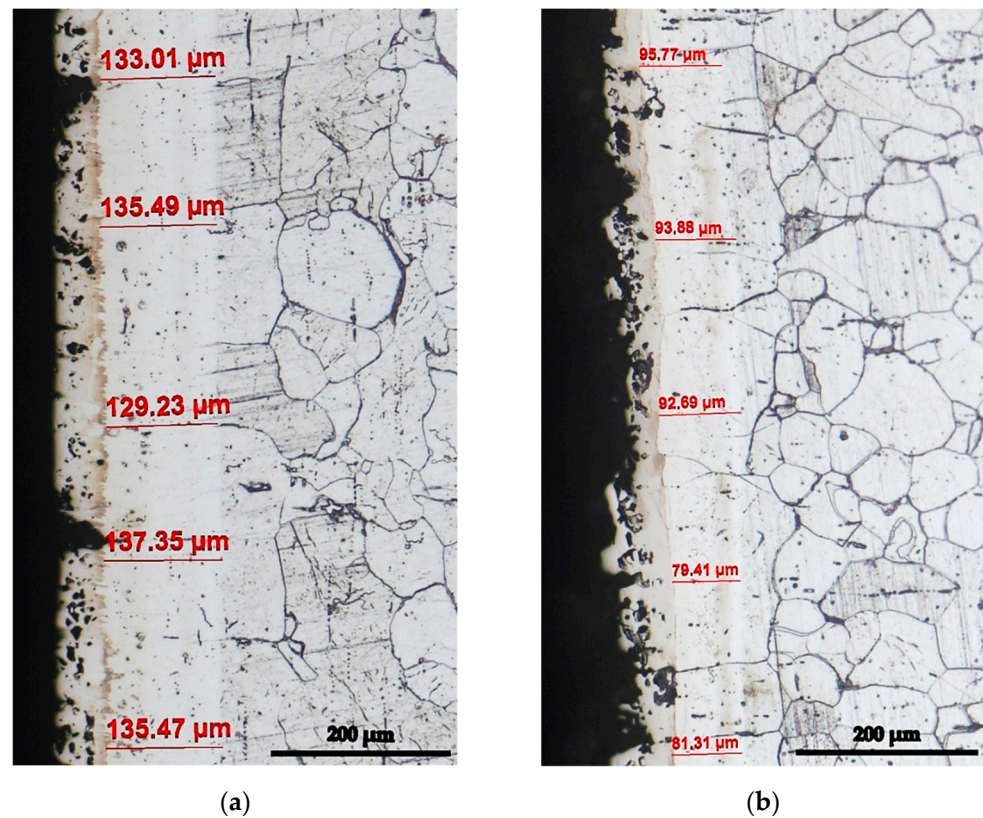


**Figure 1.** The effects of change in the growth kinetics of the free porous zone with the variation of the holding time with temperature (1150 °C) and the proportion of active component (FeSi75C) from the powdered solid mixture. Etchant: Nital 2%. (a) 1150 °C/5 h; 40% FeSi; 9% NH<sub>4</sub>Cl (exp. 3); (b) 1150 °C/1 h; 60% FeSi; 9% NH<sub>4</sub>Cl (exp. 4).

The following correlation is between the real values and the codified values of the independent parameters:

$$x_i = \frac{X_i - X_{i0}}{\Delta X_i} \quad (2)$$

where:

$x_i$ —the coded value of the independent parameter  $i$  (or  $j, k \dots ij, ik \dots ijk$ ).

$X_i$ —the natural value of the independent parameter  $i$  (or  $j, k \dots ij, ik \dots ijk$ )—Table 1.

$X_{i0}$ —the natural value of the independent parameter  $i$  (or  $j, k \dots ij, ik \dots ijk$ ) corresponding to the chosen base level (Table 1).

$\Delta X_i$ —the variation range of the independent parameter  $i$  (or  $j, k \dots ij, ik \dots ijk$ )—Table 2.

The null value corresponding to the dimension of the free porous zone in contact with the thermochemically processed surface is not always equivalent to the absence of the silicon cemented layer; this can exist, but with porosity extended to the proximity of the thermochemically processed surface. The algorithm applied to explain the regression equations (of the type of Equation (1)) is the following:

- Determination of the regression equations coefficients ( $b_0; b_i; b_j; \dots b_{ij}; b_{ik} \dots b_{ijk} \dots$ ) —Table 3.

$$b_0 = \frac{\sum_{u=1}^N y_u}{N} \quad (3)$$

$$b_{i;j} = \frac{\sum_{u=1}^N x_{(i;j)\dots} y_u}{N} \quad (4)$$

$$b_{ii...jl} = \frac{\sum_{u=1}^N x_{(ii...il)u} Y_u}{N} \quad (5)$$

where  $N$  represents the total number of experiments ( $N = 16$ ) and  $u$  is the current number of experiments.

**Table 2.** Complete factorial experiment (EFC)  $2^n > 2^4$ ; experimental conditions and results obtained.

| Factors   | T <sub>i</sub> [°C]<br>X <sub>1</sub> | T <sub>i</sub> [h]<br>X <sub>2</sub> | [%], FeSi<br>X <sub>3</sub> | [%], NH <sub>4</sub> Cl<br>X <sub>4</sub> | δ [μm]<br>Active<br>Component:<br>FeSi75C |
|---|---------------------------------------|--------------------------------------|-----------------------------|---|---|
|   |                                       |                                      |                             |   | Y   |
| Range of Variation (ΔX <sub>i</sub> )             | 100 °C                                | 2 h                                  | 10%                         | 3%  | -   |
| Higher level (X <sub>i0</sub> + ΔX <sub>i</sub> ) | (+1)/1150 °C                          | (+1)/5 h                             | (+1) 60%                    | (+1) 9%                                   | -   |
| Base level (X <sub>i0</sub> )                     | (0)/1050 °C                           | (0)/3 h                              | (0) 50%                     | (0) 6%                                    | -   |
| Lower level (X <sub>i0</sub> - ΔX <sub>i</sub> )  | (-1)/950 °C                           | (-1)/1 h                             | (-1) 40%                    | (-1) 3%                                   | -   |
| Exp.1   | (+1)/1150 °C                          | (+1)/5 h                             | (+1) 60%                    | (+1) 9%                                   | 125.59                                    |
| Exp.2   | (+1)/1150 °C                          | (+1)/5 h                             | (+1) 60%                    | (-1) 3%                                   | 301.368                                   |
| Exp.3   | (+1)/1150 °C                          | (+1)/5 h                             | (-1) 40%                    | (+1) 9%                                   | 134.11                                    |
| Exp.4   | (+1)/1150 °C                          | (-1)/1 h                             | (+1) 60%                    | (+1) 9%                                   | 88.61                                     |
| Exp.5   | (-1)/950 °C                           | (+1)/5 h                             | (+1) 60%                    | (+1) 9%                                   | 0.00                                      |
| Exp.6   | (+1)/1150 °C                          | (+1)/5 h                             | (-1) 40%                    | (-1) 3%                                   | 270.94                                    |
| Exp.7   | (+1)/1150 °C                          | (-1)/1 h                             | (+1) 60%                    | (-1) 3%                                   | 134.39                                    |
| Exp.8   | (+1)/1150 °C                          | (-1)/1 h                             | (-1) 40%                    | (+1) 9%                                   | 156.27                                    |
| Exp.9   | (-1)/950 °C                           | (-1)/1 h                             | (+1) 60%                    | (+1) 9%                                   | 137.78                                    |
| Exp.10  | (-1)/950 °C                           | (+1)/5 h                             | (-1) 40%                    | (+1) 9%                                   | 0.00                                      |
| Exp.11  | (-1)/950 °C                           | (+1)/5 h                             | (+1) 60%                    | (-1) 3%                                   | 0.00                                      |
| Exp.12  | (-1)/950 °C                           | (-1)/1 h                             | (-1) 40%                    | (+1) 9%                                   | 0.00                                      |
| Exp.13  | (-1)/950 °C                           | (-1)/1 h                             | (+1) 60%                    | (-1) 3%                                   | 0.00                                      |
| Exp.14  | (-1)/950 °C                           | (+1)/5 h                             | (-1) 40%                    | (-1) 3%                                   | 35.02                                     |
| Exp.15  | (+1)/1150 °C                          | (-1)/1 h                             | (-1) 40%                    | (-1) 3%                                   | 0.00                                      |
| Exp.16  | (-1)/950 °C                           | (-1)/1 h                             | (-1) 40%                    | (-1) 3%                                   | 0.00                                      |

**Table 3.** The calculated values of the coefficients of the regression equations are coefficients of the experimental values mentioned in Table 2.

| Coefficient       | Active Part: FeSi |
|-------------------|-------------------|
| b <sub>0</sub>    | 86.48             |
| b <sub>1</sub>    | 64.88             |
| b <sub>2</sub>    | 39.07             |
| b <sub>3</sub>    | -5.28             |
| b <sub>4</sub>    | -6.23             |
| b <sub>12</sub>   | 17.4              |
| b <sub>13</sub>   | 16.3              |
| b <sub>14</sub>   | -19.0             |
| b <sub>23</sub>   | -13.6             |
| b <sub>24</sub>   | -20.0             |
| b <sub>34</sub>   | -21.5             |
| b <sub>123</sub>  | 7.98              |
| b <sub>124</sub>  | -32.9             |
| b <sub>234</sub>  | 3.75              |
| b <sub>134</sub>  | -8.65             |
| b <sub>1234</sub> | 16.6              |

- Determination of dispersion of reproducibility of the experimental values ( $S_0^2$ ) is achieved by several experimental values obtained in identical conditions (a minimum of three values).

The calculation of the dispersion of reproducibility of the experimental values  $S_0^2$  was obtained by the values obtained in conditions corresponding to experiment no.1 (see Table 2) and those conditions where all the independent parameters are at their superior level of variation.

Through the dispersion of reproducibility, we estimated the range of confidence intervals ( $\Delta b_i$ ) where the values of the coefficients of the confidence values must be framed. In these conditions, the following values have been obtained, as presented in Table 4.

**Table 4.** Statistical verification of coefficients of regression equations.

| Parameter                         | Active Component: FeSi |            |
|-----------------------------------|------------------------|------------|
| $S_0^2$                           | 54.31                  | $t = 2.12$ |
| $S_{b_i}^2; S_{b_{ij}}^2$         | 3.394                  |            |
| $\Delta b_i; \Delta b_{ij} \dots$ | $\pm 3.905$            |            |

In Table 4  $S_{b_i;ij}^2$  represents the dispersion utilized for calculation of the coefficients  $b_i; b_{ij}; \dots b_{ijk}$

$$\Delta b_{i;ij\dots ijk} = \pm \sqrt{S_{b_i;ij\dots}^2} t_{\alpha;N} \quad (6)$$

where  $t_{\alpha;N}$  is the "Student" criterion for the significance threshold  $\alpha = 0.05$  and the number  $N$  of a degree of freedom (total number of experiments;  $N = 16$ )  $t_{\alpha;N} = 2.12$  (tabular value) [11,12].

The mathematical expression of the condition for statistical variation of the coefficients is:

$$|b_{i;ij\dots ijk}| \geq \Delta b_{i;ij\dots ijk} \quad (7)$$

The comparison of the calculated values of the coefficients of the regression equations (Table 3) with the related confidence ranges (Table 4) resulted in some of them being statistically negligible (they do not have a significant influence on the dependent parameter considered), and the particular form of the regression equation for those analyzed becomes:

A. The active component of the powdered solid medium FeSi75C

$$Y = \delta (\mu\text{m}) = 86.48 + 64.88X_1 + 39.07X_2 + 17.4X_1X_2 + 16.3X_1X_3 - 10X_1X_4 - 13.6X_2X_3 - 20X_2X_4 - 21.5X_3X_4 - 32.9X_1X_2X_4 - 8.65X_1X_3X_4 + 16.6X_1X_2X_3X_4 \quad (8)$$

The verification of the consistency of the mathematical model: The hypothesis of the consistency of the mathematical model adopted was checked using the Fischer criterion, of which the calculated value is determined through the relation:

$$F_{calc} = \frac{S_{conc}^2}{S_0^2} \quad (9)$$

where  $S_{conc}^2$  represents the dispersion of the values due to the application of the mathematical model calculated in rapport with the experimental values.

$$S_{conc}^2 = \frac{\sum_{u=1}^N (\bar{y}_u - y_{uexp})^2}{N - K'} \quad (10)$$

where  $\bar{y}_u$  and  $y_{uexp}$  represent the value calculated using the regression equations, obtained experimentally, and  $u$  represents the experience number.  $K'$  represents the number of coefficients of the regression equations at which the free element,  $b_0$ , will be added.

The calculated mathematical model is considered to be consistent (this reflects a maximum probability—the influence of the independent parameters in the analysis on the dependent parameter), for the case where the statistical verification condition is fulfilled:

$$F_{calc} < F_{tab(0.05; \nu_1; \nu_2)}$$

where  $\nu_1$  represents the number of degrees of freedom considered to calculate the consistency dispersion  $S^2_{conc}$  ( $\nu_1 = N - K'$ ), and  $\nu_2$  is the number of degrees of freedom considered to calculate the dispersion of the experimental reproducibility,  $S^2_0$  ( $\nu_2 = n - 1$ , where  $n$  represents the number of experiments performed in identical conditions;  $n = 3$  for the current situation)—Table 5.

**Table 5.** Statistical verification of the adequacy of the adopted mathematical model.

| Statistical Parameter | Active Component: FeSi75C |                 |
|-----------------------|---------------------------|-----------------|
| $F_{tabular}$         | 19.4                      |                 |
| $S^2_{conc}$          | $313.62 \cdot 10^{-4}$    | $S_0^2 = 54.31$ |
| $F_{calculated}$      | $5.77 \cdot 10^{-4}$      |                 |

The comparative analysis of the calculated values with those tabular values corresponding to the Fischer criteria (see Table 5) certifies that the calculated mathematical model, Equation (8), reflects the maximum probability and the individual and collective influences of the independent parameters considered on the dependent parameter, represented by the free porous zone of the silicon cemented layer and perfectly adherent to the support.

The graphical expressions of the regression Equation (8) are shown in Figures 2 and 3.

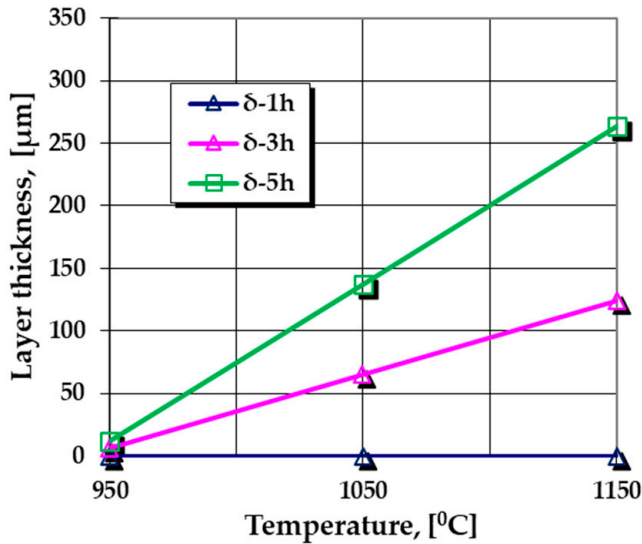
The graphical dependencies represent the graphical expressions of the regression Equation (8) for different particular situations of the processing parameters.

The graphical dependencies represent the graphical expressions of the regression Equation (8) for different particular conditions of the processing parameters.

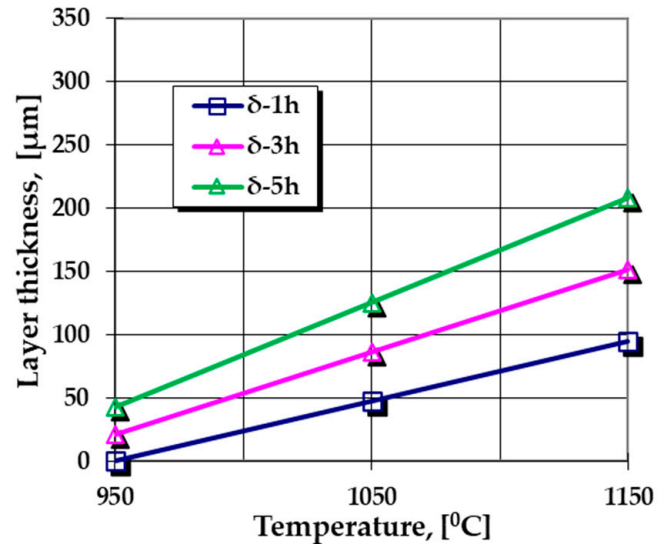
The analysis of the results obtained (see Figures 1 and 2 and regression Equation (8)) outlines the individual and cumulated effects of the independent parameters considered on the growth kinetics of the targeted zone of the silicon cemented layer obtained on high-purity iron, as follows:

- The increase in the proportion of halide, utilized as an activator of the reactions between the components of the powdered solid medium, but also as an activator of the surface of the thermochemically processed metallic product, has a significant effect, especially for high values of the active component of the medium (ferrosilicon), as is shown in Figure 2a,c. Thus, for example, for 60% FeSi75C, the effects of the increase in the proportion of halide between 3 and 9% for a constant holding time on temperature is strictly dependent on the processing temperature—at 3%  $\text{NH}_4\text{Cl}$ , the kinetics accelerates when the temperature is higher and the holding time is longer, as is shown in Figure 2d. At 9%  $\text{NH}_4\text{Cl}$ , the variation of the holding time does not influence the kinetics, regardless of the processing temperature, as is shown in Figure 2c.
- For moderate proportions of the active component (FeSi75C) in the powdered solid medium used for silicon cementation, the effects of variation of the proportion of halide in the medium may be different over time: From the kinetic accelerator to small reduced processing times, to become a brake at high values of holding time, as shown in Figure 3b, the amplitude of the effects is dependent on the proportion of halide in the media used for silicon cementation with an obvious correlation with the other parameters. The explanation of the dual characteristics is related to the ratio between the intensities with which the effects of activating the reactions between the environmental components and those of cleaning/activating the metal surface subjected to thermochemical processing are manifested.

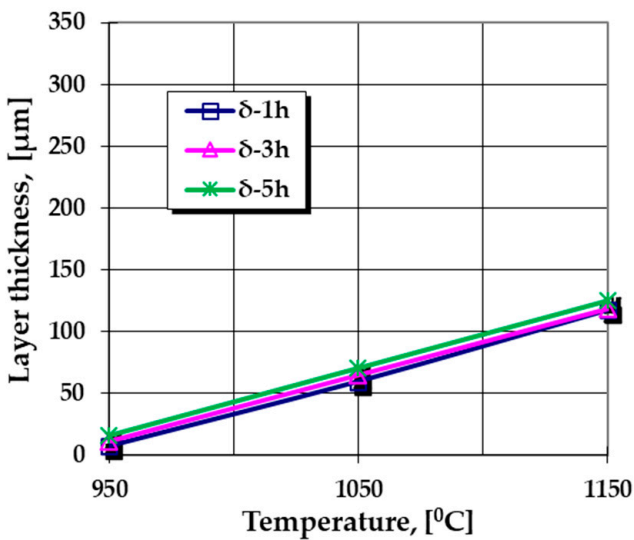
The change in the growth kinetics of silicon-cemented layers depending on the processing temperature must be strictly correlated with the variation of the diffusion coefficient of silicon in the iron matrix at a certain temperature. Thus, if at 1223 K (the lower limit of the temperature variation range chosen in the research program), the diffusion coefficient of silicon in iron is  $5.71 \times 10^{-7} \text{ m}^2/\text{s}$ , according to Mehrer et al. [16], Batz et al [17], and Mirani et al. [18], at 1423 K (the upper limit of the temperature range chosen in research program), this increases by an order of magnitude, reaching  $2.42 \times 10^{-6} \text{ m}^2/\text{s}$ , according to the same references.



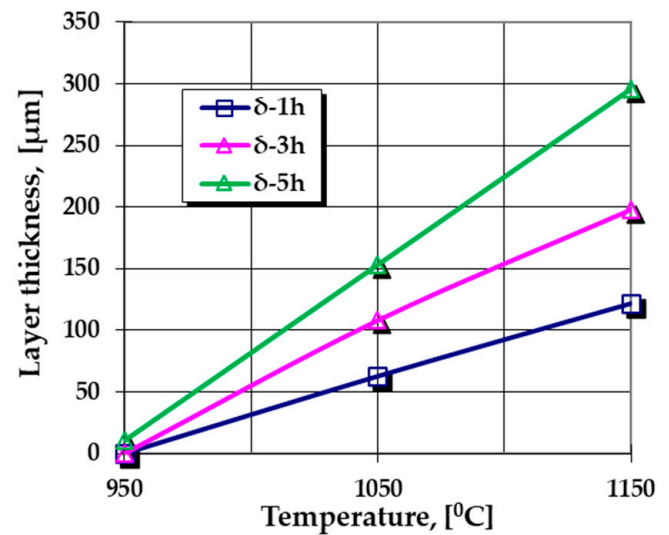
(a) 40%FeSi; 3%NH<sub>4</sub>Cl



(b) 50%FeSi; 6%NH<sub>4</sub>Cl



(c) 60%FeSi; 9%NH<sub>4</sub>Cl



(d) 60%FeSi; 3%NH<sub>4</sub>Cl

**Figure 2.** The change in the growth kinetics of the silicon cemented layer (dense and adherent zone) generated by the variation of temperature, the holding time on temperature, and the proportion of ferrosilicon (FeSi75C), namely the proportion of ammonia chloride in the solid powdered mixture utilized.

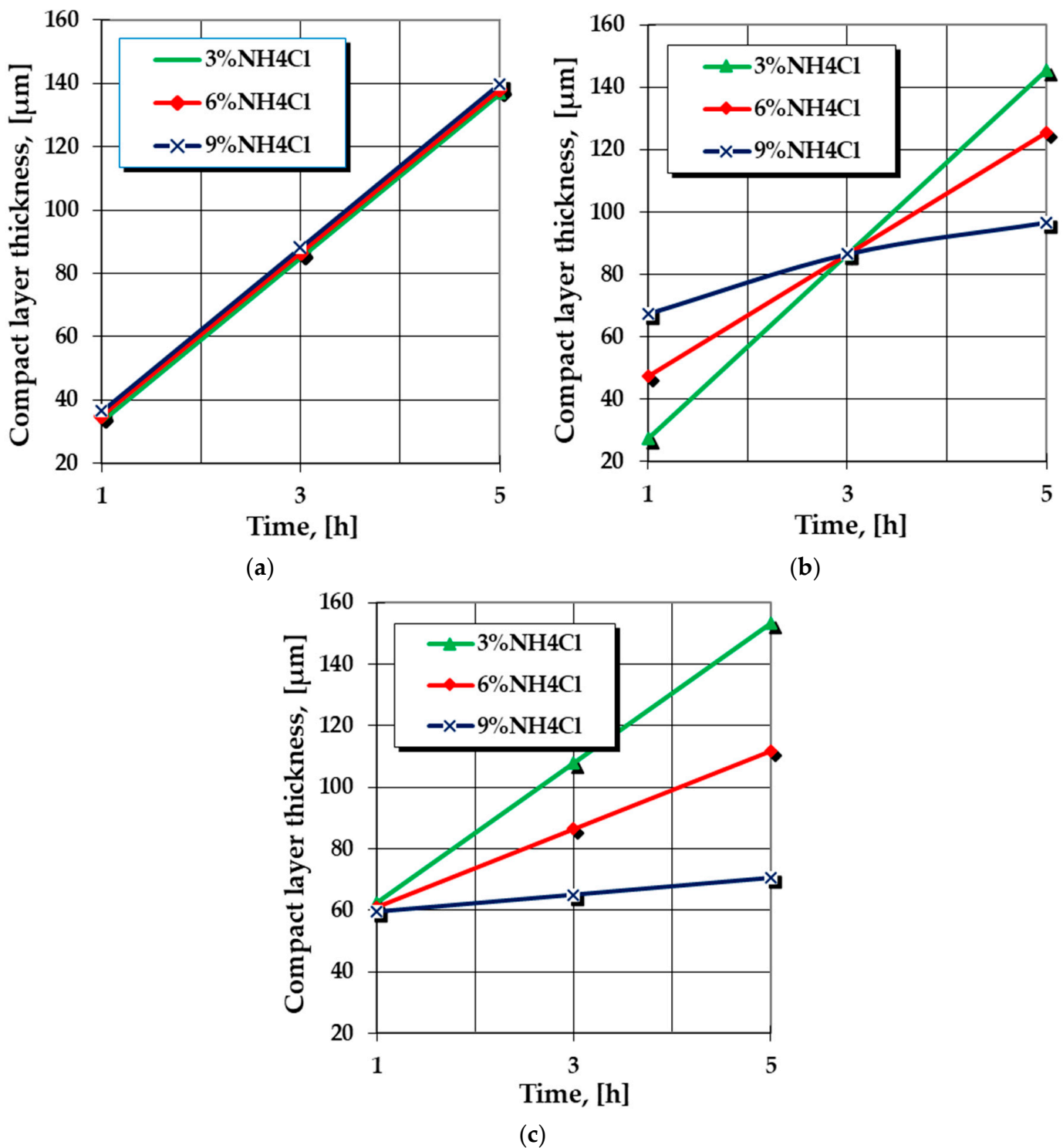


**Figure 3.** The change of growth kinetics of the silicon cemented layer (compact and adherent) is generated by the variation of the holding time on temperature, the ferrosilicon (FeSi75C) proportion, and the ammonia chloride in the powdered solid mixture utilized. (a) T = ct = 1050 °C; %FeSi = ct = 40%; (b) T = ct = 1050 °C; %FeSi = ct = 50%; (c) T = ct = 1050 °C; %FeSi = ct = 60%.

#### 4. Discussion

To fully understand the results obtained and define their trends, a thorough analysis of the reactions between the components of the medium used for silicon cementation is necessary.

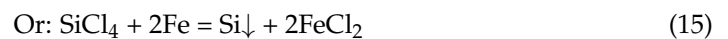
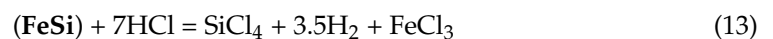
Thus, the sequence of reactions in the medium, at the media–metal surface interface, and in the adsorbed state is reproduced below:

| Active component | Activator          | Ballast Element<br>(Dispersion component) |
|------------------|--------------------|---|
| FeSi75C          | NH <sub>4</sub> Cl | Al <sub>2</sub> O <sub>3</sub>            |



↓

N<sub>2</sub>



The analysis of the chemistry of the reactions that occurred between the powdered solid media components utilized for silicon cementation, as shown in the sequence of Equations (11)–(21), together with the information resulting from the thermodynamical study on their thermal effects and the probability of development in the right sense, led to the following conclusions:

- The silicon appears in the superficial zones of the thermochemically processed metallic products following a sequence of chemical reactions, either occurring often between its chlorides adsorbed in the superficial layers and the iron atoms (Equations (15) and (17)), or in the surface proximity following the reactions between its chlorides and the hydrogen resulting from the decomposition of the ammonia chloride (Equations (11) and (19)), etc.
- Most of the reactions that occurred between the components of the powdered solid media utilized for silicon cementation develop with heat release (significant thermal effect).
- The development of silicon chlorides is dependent on the ammonia chloride among the components of the powdered solid media and its decomposition at the processing temperature—Equation (11); however, the increase in the proportion of this component can have adverse effects such as the cleaning/corrosion of the surface, an aspect that must be considered when dosing its proportion.
- The appearance of Si in a free state in the silicon cementation media, as defined in Equation (19), is likely to be determined from the thermodynamic point of view (see Figure 4), as is the formation of a nitride of Si<sub>2</sub>N type after a reaction of the following type:



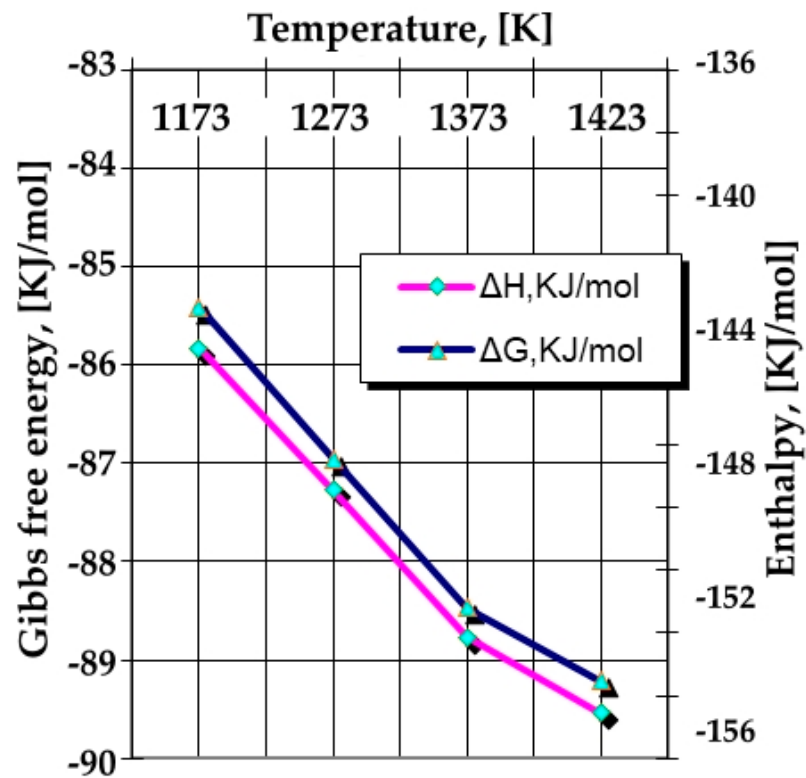


**Figure 4.** The evolution of the main thermodynamical properties specific to Equation (22) with temperature, was obtained with the help of Outotec's HSC 6.12 Chemistry Software [19].

Note that the nitrogen in the atomic state can be obtained by thermocatalytic decomposition of ammonia at the metal product interface, as is shown in Equation (12).

Concomitant with the thermocatalytic decomposition of ammonia at the interface of the metal surface of the product subjected to thermochemical processing, an ionization of its molecules with the formation of anionic complexes of the  $\text{NH}_3^-$  type is also very likely. According to the ionic mechanism of adsorption, the formation of such anionic complexes and their adsorption in the electric double layer of the metal surface is extremely possible at a temperature at which cementation with silicon takes place [20,21]. The formation of the anionic complex  $\text{NH}_3^-$  after the reaction of  $\text{NH}_3 + e = \text{NH}_3^-$  is extremely likely and is achieved with an energy release in the order of 2.8 eV [22]. This energy is transferred to the electrons from the electric double layer of the surface of the metal matrix subjected to processing. The energy required for the electrons to overcome the potential barrier at the level of the metal surface and continue the ionization process of the ammonia molecules is composed of the thermal energy of the electrons in the metal ( $\sim 0.16$  eV at 1273 K) and the kinetic energy of the ammonia molecules transferred to the electrons from the electric double layer upon impact with the metal surface ( $\sim 0.1$  eV) to which the 2.8 eV released at the time of the formation of the anionic complex is added. The size of the potential barrier in the case of the iron matrix, which contains a layer in the order of several microns of  $\text{Fe}_2\text{O}_3$ , is in the order of 3 eV, a value lower than the total energy of the electrons [20]. The manifestation of the ionic mechanism of the formation and adsorption of the  $\text{NH}_3^-$  anionic complex is confirmed by the results of the investigations regarding the concentration of nitrogen in the silicon cemented layer, as is shown in Figure 5.

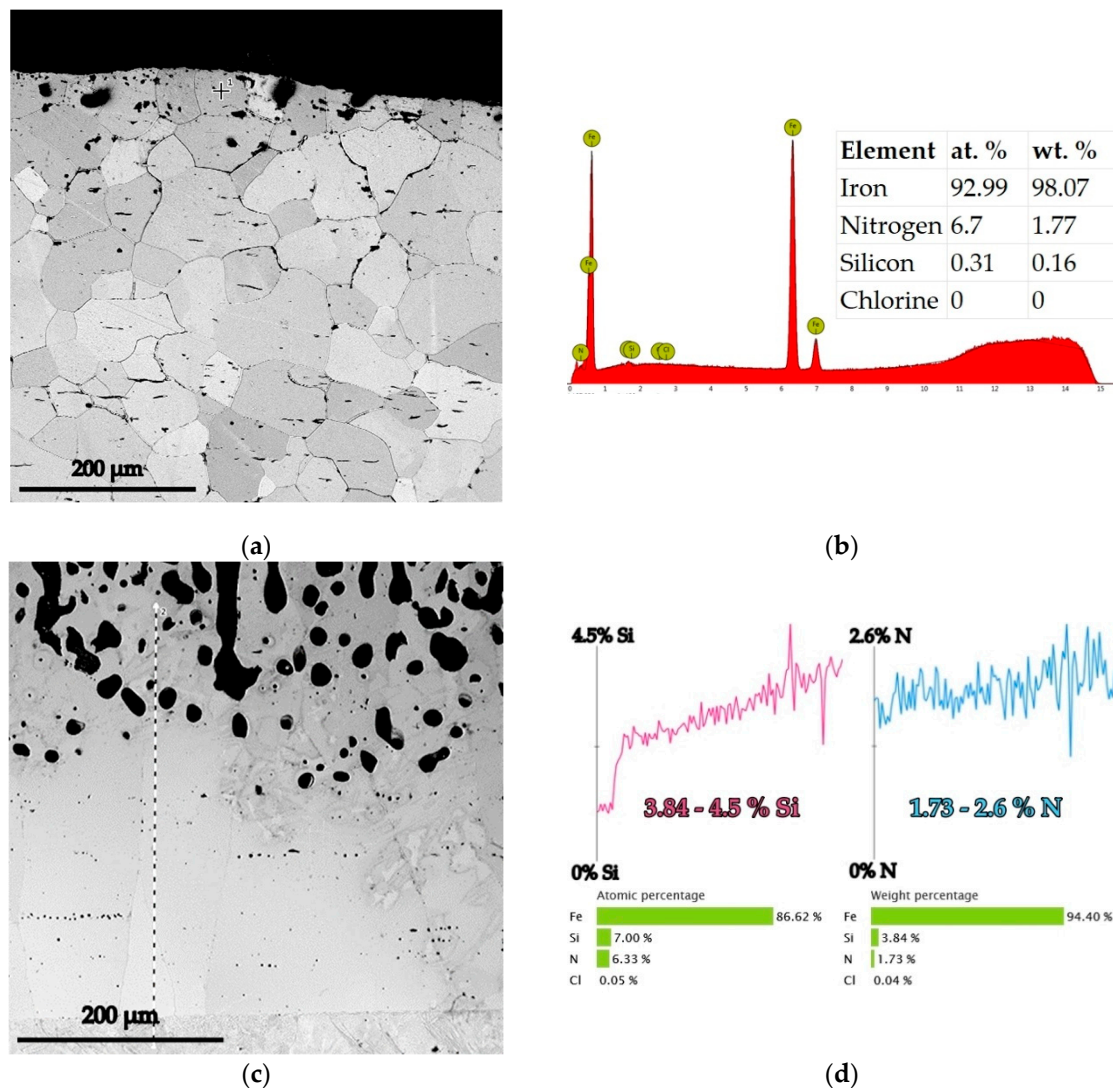


**Figure 5.** The change in the growth kinetics of the silicon cemented layer (dense and adherent zone) generated by the variation of temperature, the holding time on temperature, and the proportion of ferrosilicon (FeSi75C), namely the proportion of ammonia chloride in the solid powdered mixture utilized. (a) 950 °C/5 h; 60% FeSi75C; 3% NH<sub>4</sub>Cl; (b) Max. values of the %Si and %N in layer; (c) 1150 °C/5 h; 60% FeSi75C; 3% NH<sub>4</sub>Cl; (d) Variation of the Si (red line) and the N (blue line) in the Si cemented layer.

In the case of silicon nitride (Si<sub>2</sub>N), for the formation of the cationic complex Si<sub>2</sub>N<sup>+</sup>, energies in the order of 6.4 eV are required [23], which are impossible to ensure under the conditions in which the thermochemical processing takes place, so it is concluded that the only source of nitrogen in the layer is the presence of the complex anions NH<sub>3</sub><sup>-</sup>. It seems that the formation of Si<sub>2</sub>N compounds, very likely from a thermodynamic point of view, does not contribute anything to the level of silicon content in the cemented layer.

It can be concluded that saturation by the diffusion of the superficial areas of thermochemically processed Fe-ARMCO in a powdery solid medium containing ferrosilicon FeSi75C, Al<sub>2</sub>O<sub>3</sub>, and halide NH<sub>4</sub>Cl is based on both an atomic mechanism of adsorption, which ensures the enrichment mainly with silicon, and an ionic one, which mainly ensures nitrogen enrichment.

X-ray microanalysis performed using an energy dispersive spectrometer (EDS), in the areas adjacent to the thermochemically processed surfaces, confirms the presence of N

alongside the Si adsorbed and diffused in the layer in different concentrations, depending on the temperature and type of active component, as is shown in Figure 5.

The regression Equation (8) allows us to make a prediction, with a probability of 95%, by calculating the dimension of the non-porous layer in direct contact with the metal support subjected to processing. It allows us to estimate how the thermal, temporal, and chemical parameters of the processing can be correlated to obtain certain dimensions of the zone of interest of the layer, or how this can be compensated (if this is possible) by the partial presence of a certain parameter (for example, how can a certain value of the temperature or the holding time at the temperature be compensated), if technological reasons require these, by changing the level of the other parameters.

The cited literature [1] shows that an increase in the carbon concentration in the superficial areas of the products subjected to silicon cementation is very likely to determine a decrease in the differences between the partial diffusion coefficients of Si in Fe and the reverse, of Fe in Si, and thereby diminish the probability of diffusion porosity occurring (reducing the magnitude of the development of the Kirkendall–Frenkel phenomenon).

It is known that the dimensions of the Si diffusion coefficient in the metal matrix are strictly dependent on the activity of the media used for thermochemical processing, the processing temperature, and the chemical composition of the metal matrix. The presence of carbon determines a barrier to the formation process of the total silicon cemented layer and an increase in the free porous zone in the layer (it decreases the value of the diffusion coefficient of Si in Fe and, implicitly, the tendency of porosity formation due to the decrease in the intensity of the appearance of the Kirkendall–Frenkel effect); the strongest influence due to the variation of the carbon proportion on the kinetics layer growth in general and the free porous zone, in particular, is shown in the range of concentrations of 0.05–0.2% mass [1].

The research on the microstructure of the silicon cemented layer in the case of high purity (Fe-ARMCO) is presented in Figure 6 and highlighted the intensity at which the Si diffusion process is carried out on the boundary of the austenite grains. The etching with 3% Nital reagent revealed both the presence of ferrite with silicon separated on the grain boundaries during cooling from the silicon cementation temperature (darker areas) and the former austenite grain boundaries (lighter).

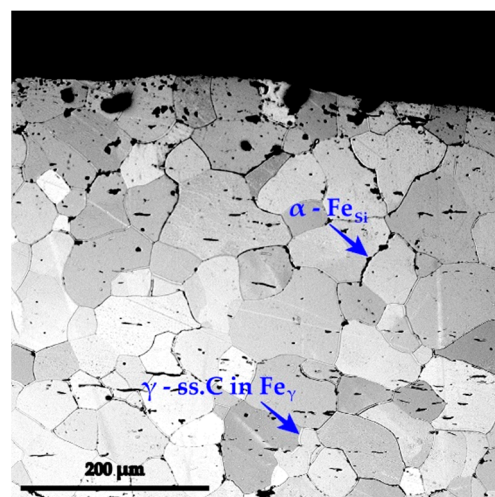


**Figure 6.** Microstructure detail revealing the magnitude and the effects of the diffusion coefficient on the grain size during silicon cementation; processing conditions: 950 °C/5 h; 40% FeSi75C; 9% NH<sub>4</sub>Cl; rest Al<sub>2</sub>O<sub>3</sub>; etchant: Nital 3%.

The microhardness tests performed on high-purity iron samples cemented by silicon under various processing conditions have shown a maximum microhardness of approximately 470  $\mu HV_{0.05}$ .

## 5. Conclusions

1. The statistical processing of the obtained experimental data led to the conclusion that ferrosilicon with higher than 60% silicon concentrations (FeSi75C) represent a significant active component, especially in the range of temperatures higher than 1100 °C.
2. Both the atomic adsorption mechanism responsible for silicon saturation and the ionic mechanism responsible for nitrogen saturation contribute to the formation of the silicon-cemented layer in a powdery solid environment consisting of FeSi75C-Al<sub>2</sub>O<sub>3</sub>-NH<sub>4</sub>Cl.
3. During the holding time at the silicon cementation temperature, the Si<sub>2</sub>N silicon nitride synthesis reaction is very likely from a thermodynamic point of view, but its presence seems not to influence the final silicon content of the layer.
4. The maximum thickness of the silicon cemented layer zone free of porosity, in direct contact with the substrate, namely, Fe-ARMCO, subjected to processing, is obtained by associating a proportion of the active component as high as possible (60%) and as low as possible (at the lower limit imposed of the programming method chosen, namely, 3%) for the component with the role of activator of the reactions in the powdered solid media. For moderate proportions of the active component (FeSi75C) in the powdered solid media used for silicon cementation, the variation of the proportion of halide in the media may register different effects over time, becoming a kinetic accelerator for low processing times or a barrier for high processing times. Thus, at reduced holding times, the maximum kinetic is recorded by the mixtures that have the highest proportion of halide (approximately 9%), and once the holding time increases, the maximum effect will be recorded by the mixtures with low concentrations of halide in the powdery mixture (approximately 3%).
5. The calculated and statistically verified mathematical models allow anticipation via the calculation of the modality of combining the parameters with a significant influence on the growth kinetics of the free porous zone of the silicon cemented layer in powdered solid media.

**Author Contributions:** Conceptualization, M.O.C., M.B. and C.M.C.; methodology, M.O.C., M.B. and M.D.M.; software, M.O.C.; validation, M.O.C., M.D.M. and M.B.; formal analysis, C.M.C., M.D.M. and D.D.; investigation, M.O.C., M.B., C.M.C. and M.D.M.; resources, M.O.C. and M.B.; data curation, M.D.M., D.D., M.B. and M.O.C.; writing—original draft preparation, M.O.C., M.B. and D.D.; writing—review and editing, M.O.C., M.B., D.D. and M.D.M.; visualization, M.O.C., M.B. and M.D.M.; supervision, M.O.C., M.B. and C.M.C.; project administration, M.O.C., M.B. and M.D.M. All authors have read and agreed to the published version of the manuscript.

**Funding:** This research received no external funding.

**Data Availability Statement:** The study did not report any data.

**Conflicts of Interest:** The authors declare no conflict of interest. The funders had no role in the design of the study; in the collection, analyses, or interpretation of data; in the writing of the manuscript, or in the decision to publish the results.

## References

1. Lakhtin, I.M.; Arzamasov, B.N. *Thermochemical Treatments of Steels*; Metallurgiya (Metallurgy Publishing House): Moscow, Russia, 1985; pp. 141–154. (In Russian)
2. Minkevici, A.N. *Thermochemical Treatments of Metals and Alloys*; Tehnica, Ed.; Technical Publishing House: Bucharest, Romania, 1968; pp. 295–308. (In Russian)
3. Barey, D.M.O.A. Concentrations and Reactions of Iron in Crystalline Silicon after Aluminum Gettering. Ph.D. Thesis, Georg-August University Goettingen, Göttingen, Germany, 29 November 2011; p. 52. (In German).
4. Kubachewski von Goldbeck, O. Fe-Si Iron-Silicon. In *IRON-Binary Phase Diagrams*; Springer: Berlin/Heidelberg, Germany, 1982; pp. 136–139. [[CrossRef](#)]
5. Hauser, H.H. *Coatings of High-Temperature Materials*; Samsonov, G.V., Epik, A.P., Eds.; Springer Science & Business Media: New York, NY, USA, 1966; Part 1; pp. 59–62. [[CrossRef](#)]

6. Dueva, T.Y. *Herald of the Machine Industry*; USSR: Moscow, Russia, 1937; Volume 16–17, p. 35. (In Russian)
7. Haslam, R.T.; Carlsmith, L.E. The Cementation of Iron by Silicon. *Ind. Eng. Chem.* **1924**, *16*, 1110–1113. [[CrossRef](#)]
8. Balandin, Y.A.; Kolpakov, A.S. Diffusion Siliconizing in a Fluidized Bed. *Metal Sci. Heat Treat.* **2006**, *48*, 127–130. [[CrossRef](#)]
9. Fitzer, E. The siliconizing of steel as a solid state reaction. *Arch. Das Eisenhuettenwesen* **1954**, *25*, 455–463. [[CrossRef](#)]
10. Leahovici, L.S.; Vorosnina, L.G.; Şcerbakov, E.R.D.; Panin, G.G. *Siliconization of Metals and Alloys*; Tehnica, N.I., Ed.; Scientific and Technical Publishing House: Minsk, Russia, 1972; pp. 193, 255–261. (In Russian)
11. Taloi, D.; Florian, E.; Bratu, C.; Berceanu, E. *Optimization of Metallurgical Processes*; Pedagogica, D.S., Ed.; Didactic and Pedagogical Publishing House: Bucharest, Romania, 1983; pp. 79–85. (In Romanian)
12. Dimitriu, S.; Taloi, D. *Mathematical Modeling Methods of Technological Processes*; Printech, Ed.; Printech Publishing House: Bucharest, Romania, 2014; pp. 194–206. (In Romanian)
13. Hics, C. *Basic Principles of Experiment Planning*; Izd.Mir (World Publishing House): Moscow, Russia, 1967. (In Russian)
14. Himmelbau, D. *Process Analysis by Statistical Methods*; Izd.Mir (World Publishing House): Moscow, Russia, 1975. (In Russian)
15. Johnson, N.; Leone, F. *Statistics and Experimental Programming in Technology and Science. Data Processing Methods*; Izd.Mir (World Publishing House): Moscow, Russia, 1980. (In Russian)
16. Mehrer, H.; Eggersmann, M.; Gude, A.; Salamon, M.; Sepiol, B. Diffusion in intermetallic phases of the Fe-Al and Fe-Si systems. *Mater. Sci. Eng. A* **1997**, *239–240*, 889–898. [[CrossRef](#)]
17. Batz, W.; Mead, H.V.; Birchenall, C.E. Diffusion of Silicon in Iron. *J. Met.* **1952**, *10*, 1070. [[CrossRef](#)]
18. Mirani, H.V.M.; Maaskant, P. Diffusion of Si in Fe-Si Containing 8 to 11 at% Si. *Phys. Status Solidi A* **1972**, *14*, 521–525. [[CrossRef](#)]
19. *HSC Chemistry Software*, Version 6.12; Outotec Research Oy: Pori, Finland, 2007.
20. Cojocaru, M.O. Nitriding in an Electrostatic Field. Ph. D. Thesis, Moscovskii Avto-Dorojnii Institut MADI (Moscow Road Vehicle Institute), Moscow, Russia, 1976. (In Russian).
21. Cojocaru, M.O.; Ciuca, I.; Druga, L.N.; Cosmeleata, G. Empirical Exposition of the Adsorption's Ionic Mechanism on Gaseous Nitriding. *Surf. Eng. Appl. Electrochem.* **2008**, *44*, 63–68. [[CrossRef](#)]
22. Vedenev, V.I. *Breaking Energy of Chemical Bonds. Ionization Potentials and Electron and Proton Affinity*; Izd. AN-SSSR (SSSR Publishing House): Moscow, Russia, 1962. (In Russian)
23. Paukstisand, S.J.; Gole, J.L. The Ionization Potential of  $\text{Si}_2\text{N}$  and  $\text{Si}_2\text{O}^+$ . *J. Phys. Chem. A* **2002**, *106*, 8435–8441. [[CrossRef](#)]

**Disclaimer/Publisher's Note:** The statements, opinions and data contained in all publications are solely those of the individual author(s) and contributor(s) and not of MDPI and/or the editor(s). MDPI and/or the editor(s) disclaim responsibility for any injury to people or property resulting from any ideas, methods, instructions or products referred to in the content.